ELSEVIER

Ultrasonics 38 (2000) 604–608

Some aspects of AE application in tool condition monitoring

Krzysztof Jemielniak *

Warsaw University of Technology, Narbutta 86, 02-524 Warsaw, Poland

Abstract

Acoustic emission (AE) is rather a well-known form of non-destructive testing. In the last few years the technology of the AE measurement has been expanded to cover the area of tool condition monitoring. The paper presents some experience of Warsaw University of Technology (WUT) in such applications of AE. It provides an interpretation of common AE signal distortions and possible solutions to avoid them. Furthermore, a characteristic study of several different AE and ultrasonic sensors being used in WUT is furnished. Evaluation of the applicability of some basic measures of acoustic emission for tool condition monitoring is also presented in the paper. Finally paper presents a method of the catastrophic tool failure detection in turning, which uses symptoms other than the direct magnitude AE_{RMS} signal. The method is based on the statistical analysis of the distributions of the AE_{RMS} signal.

Keywords: Acoustic emission; Tool condition monitoring

1. Introduction

Rising labour cost makes production automation an important priority in the major industrial countries. One of the most important factors limiting the progress in introduction of unattended machine tool operation is tool condition monitoring (TCM). Numerous different phenomena can be employed for this purpose and a variety of sensor types are available on the market, e.g. Refs. [1–4]. Despite a growing number of publications presenting new, elegant methods of raw AE signal processing, the methods have not been applied in industrial practice so far, where rather simple methods prevail, utilising the demodulated (usually AE_{RMS}) signal [3]. However, existing tool condition monitoring systems, based on AE measurements, are still not considered reliable enough. Therefore it seems worthwhile to go back to some basic consideration concerning the AE signal processing and evaluation.

2. AE signal processing and interpretation

2.1. Measuring chain

The typical procedure of AE signal processing in metal cutting follows the pattern shown in Fig. 1. The piezoelectric AE sensor is usually placed as close as possible to the cutting zone. Low frequency noise components, which are inevitably present in AE signal, are considered to be not correlated with tool's condition and hence useless. In addition, they can be of high amplitude forcing usage of lower signal amplification. Therefore those components should be eliminated (high-pass filtered) at the earliest possible stage of signal processing, just after inevitable buffering. Sometimes the AE signal is then fed through a low-pass filter to get rid of the high frequency noise components due to electric sparks, etc. or to avoid aliasing. The raw AE signal (AE_{raw}) can be demodulated in the form of the mean value or RMS (AE_{RMS}) to obtain a low frequency variable, so it can be recorded or processed with conventional, less expensive signal processing equipment.

Fig. 2 presents AE_{raw} signal obtained from the broad band transducer Brüel & Kjær 8312 without filtering, when cutting carbon steel 45 with conventional carbide P30 worn out insert. The long view (Fig. 2(a)) shows three bursts of nearly the same maximum amplitude. In demodulated signal (analogue AE_{RMS}, Fig. 2(b)) the third burst reaches the highest value. Fragments marked with black rectangles under both figures are shown in Fig. 2(c), and their amplitude spectra are presented in Fig. 2(d). The figures reveal the existence of a dominant low frequency component. It was caused by some mechanical disturbances, and consequently should be filtered out as irrelevant to tool wear. Of course in the

* Tel.: +48-22-6608-656; fax: +48-22-8490285.
E-mail address: k.jemielniak@wip.pw.edu.pl (K. Jemielniak)

0041-624X/00/$ - see front matter
PII: S0041-624X(99)00195-X

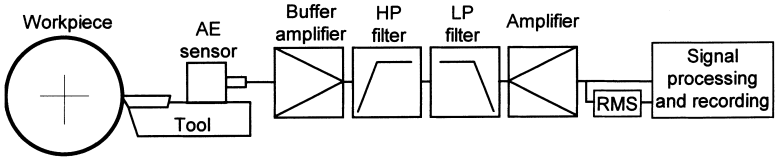

Fig. 1. Typical procedure of AE signals processing in metal cutting.

AE_{RMS} signal low and high frequency components cannot be distinguished, making need for the filtering even more imperative. Fig. 3 presents results of high-pass (150 kHz) and low-pass (500 kHz) filtering of the signal from Fig. 2. Only two of the three bursts visible in Fig. 3 remained here and the second is much lower then the first. The third, largest burst visible in Fig. 3 has just disappeared. Now the amplitude spectra consist of components only from the frequency range of interest.

2.2. AE signal distortion

The signals originating from the cutting zone can be very strong. Because of the characteristics of pre-processing units, such high amplitude signals sometimes cause overloading of the preamplifier and distortion of the signal. This can often result in a misleading evaluation of the data. Fig. 4 presents examples of distorted AE signals received from two different sensors and pre-processing units. The first was a typical laboratory transducer, and saturation of the signal (left figure) indicates a simple overloading of the amplifier. Moreover in the both signals another, less obvious, distortion can be seen – the AE signal temporarily vanishes. Similarly distorted signals have been observed in results presented by several laboratories, so a close look at it seems worthwhile.

To determine possible causes of the AE signal distortion shown in Fig. 4, let us consider what would have happened if the signal discussed in Figs. 2 and 3 had been four times stronger. At first, it would overload the buffer amplifier resulting in characteristic signal saturation – see Fig. 5(a). Those parts of the signal in which a low frequency component was dominant became rec-

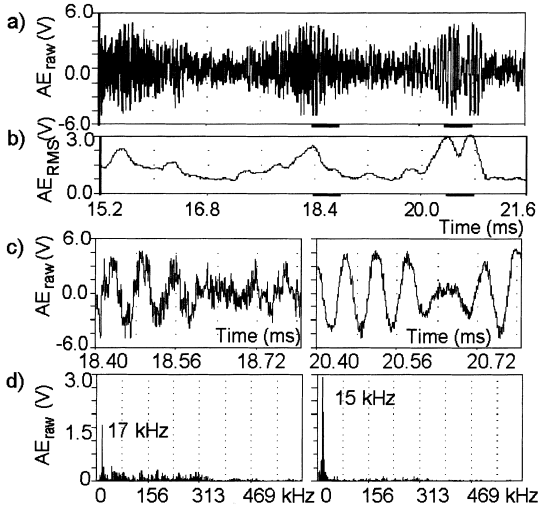

Fig. 2. AE signal obtained from Brüel & Kjær 8312 transducer: a long view (a), RMS value of the signal (b), selected fragments of the raw signal (c) and their spectra (d).

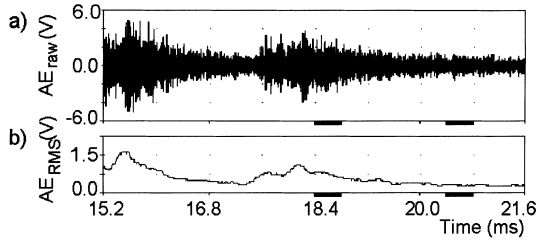

Fig. 3. AE signal from Fig. 2 after filtering (HPF 150 kHz, LPF 500 kHz): a long view (a), RMS value of the signal (b).

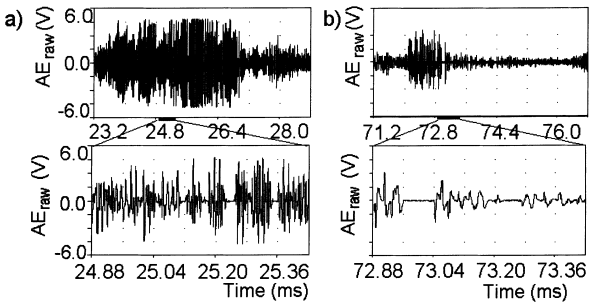

Fig. 4. Examples of distorted AE signals obtained from: (a) Brüel & Kjær 8313 sensor with 2637 preamplifier equipped with 200 kHz octave bandwidth filter, (b) Kistler 8152A1 sensor with a Kistler piezotron coupler 5125A equipped with HPF 50 kHz and LPF 1 MHz.

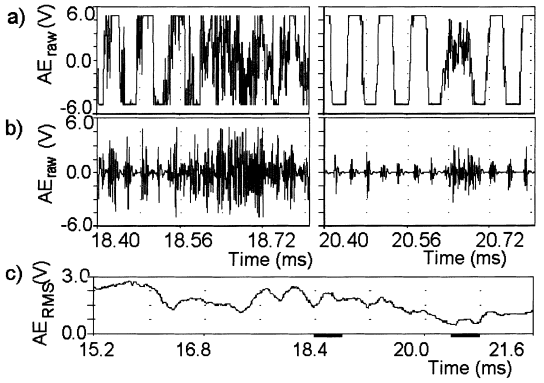

Fig. 5. AE signal from Fig. 3 after quadruple amplification (a), and filtering: selected fragments of the signal (b), RMS value of the signal (c).

tangular after quadruple amplification. After following filtering this signal by LPF 500 kHz and HPF 150 kHz it appeared that temporary vanishing of the AE signal is a result of filtering of the saturated, rectangular signal of the low frequency major component (Fig. 5(b)). Finally, no signal distortion can be observed in the AE_{RMS} signal (Fig. 5(c)), which also reaches no more than a half of the correct value, and its shape barely resembles the actual signal (Fig. 3(b)). Such signals must be considered as completely distorted, and thus useless. Therefore the gain of the buffer amplifier should be as small as possible, and any further necessary amplification should be done after signal filtering.

To avoid the signal distortion presented in Fig. 4(a), the Brüel & Kjær preamplifier type 2637 used in WUT was modified by lowering its gain by 10 (20 dB).

2.3. Calibration of AE transducers

There has been a discussion about which of the AE sensor calibration methods is absolute and the most effective. Perhaps the most easy to apply, still very reliable, is the method after Nielsen-Hsu [5], based on the breaking of a pencil lead on a steel plate. As the duration of the signal generated is very short the frequency response of the received signal waveform can be assumed as the amplitude characteristic of the sensor (and signal processing circuit). Characteristics of five sensors obtained this way in WUT are presented in Fig. 6. It can be seen that the frequency response of B&K 8312 (curve 1) is relatively high, reaching some 150 mV at ~500 kHz. The preamplifier gain in this case can be considered as a reference. The characteristic of the B&K 8313 resonance transducer with a B&K 2637 preamplifier equipped with a 200 kHz OBF (curve 2 in Fig. 6) indicates the same maximum value, even though it corresponds to a lower frequency (~125 kHz). Employment of this measuring equipment eliminated the low frequency components of the AE burst signal, leaving only the useful band. However, the signal can be still too strong, causing overload of the preamplifier and signal distortion shown in Fig. 4. The first way to avoid it is lowering the gain of the B&K 2637 buffer amplifier by 10 (Fig. 6 curve 3). Another is the application of the B&K 8314 transducer (resonance frequency at 800 kHz) with an original B&K 2637 preamplifier equipped with 200 kHz OBF which was primarily designed to use with the B&K 8313 transducer, thus, 'unsuitable' (curve 4). Finally, the characteristic of the Kistler 8152A1 sensor used with a Kistler 5125A piezotron coupler (curve 5) indicates that this preamplifier also has too high an amplification for AE measurement in close vicinity of the cutting zone, and can cause the signal distortion.

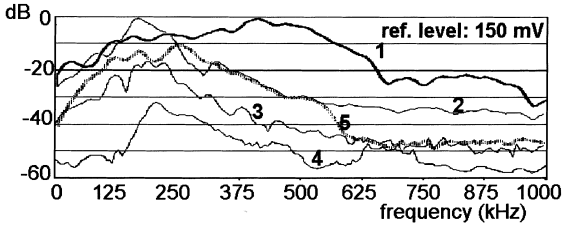

Fig. 6. Characteristics of AE sensors: curve 1, B&K 8312; curve 2, B&K 8313+2637 original preamplifier; curve 3, B&K 8313+2637 modified preamplifier; curve 4, B&K 8314+2637 original preamplifier; curve 5, Kistler 8152A1+5125A preamplifier. Note: the B&K 2637 preamplifier is equipped with a 200 kHz octave band filter.

3. Assessment of AE measures feasibility for tool wear monitoring

Measurements of AE originating from the cutting process are increasingly being utilised to diagnose tool wear especially in research laboratories. However, no success has been achieved so far in establishing any standard AE measures or methods of their recording and processing. A choice of the AE measures, which can be used for tool condition evaluation is dependent on the availability of the measuring equipment rather than on any rational analysis. AE depends not only on the tool wear, but also on a variety of other parameters such as type of wear, tool geometry, cutting conditions, cutting material and work material. Moreover, tool wear versus signal magnitude relationship is very complex and has a statistical rather than strict, predictable nature. Let us consider the applicability of some basic measures of AE for tool condition monitoring while turning steel 45 (180 HB) with TiN+TiC coated sintered carbide [6]. Crater depth (KT) was selected as the tool wear measure. Cutting parameters applied were as follows: cutting speed $v_c = 180–280$ m min^{-1}, feed $f = 0.24–0.33$ mm rev^{-1}, depth of cut $a_p = 2.5$ mm. A Brüel & Kjær 8313 AE sensor was fixed on the upper surface of the tool post. The AE_{raw} and analogue AE_{RMS} signals were recorded on a hard disk in a digital form and the files were subsequently processed to following five groups of AE measures:

- the average value ($\overline{AE}_{raw}$) and the standard deviation (s_{raw}) of the absolute value of the raw signal ($|AE_{raw}|$);
- the pulse rate (pr_1–pr_3) and the pulse width (pw_1–pr_3), that is the number of times AE_{raw} exceeds pre-set thresholds (100, 200 and 300 mV respectively) per second and the percentage of time during which AE_{raw} remains above each threshold;
- the power of the AE_{raw} signal in specific frequency ranges ($m_2 = 62.5–125$ kHz, $m_3 = 125–187.5$ kHz, $m_4 = 187.5–250$ kHz, $m_5 = 250–312.5$ kHz and $m_6 = 312.5–375$ kHz) and within its entire spectrum (m_0);
- the average value ($\overline{AE}_{RMS}$) and standard deviation (s_{RMS}) of the AE_{RMS} signal;

- the burst rate (br_1–br_3) and burst width (bw_1–bw_3), that is a number of times the AE_{RMS} signal exceeds pre-set thresholds (100, 200 and 300 mV respectively) per second and the percentage of time it remains above each threshold.

The chosen AE measures are presented in Fig. 7. The AE signal and all its measures were fairly low until the tool coating was worn out. Then all of them rose sharply. Influence of the cutting conditions was hardly visible.

In order to assess a connection between AE measures and tool wear (KT), appropriate correlation coefficients are calculated and presented in Table 1. A low r value

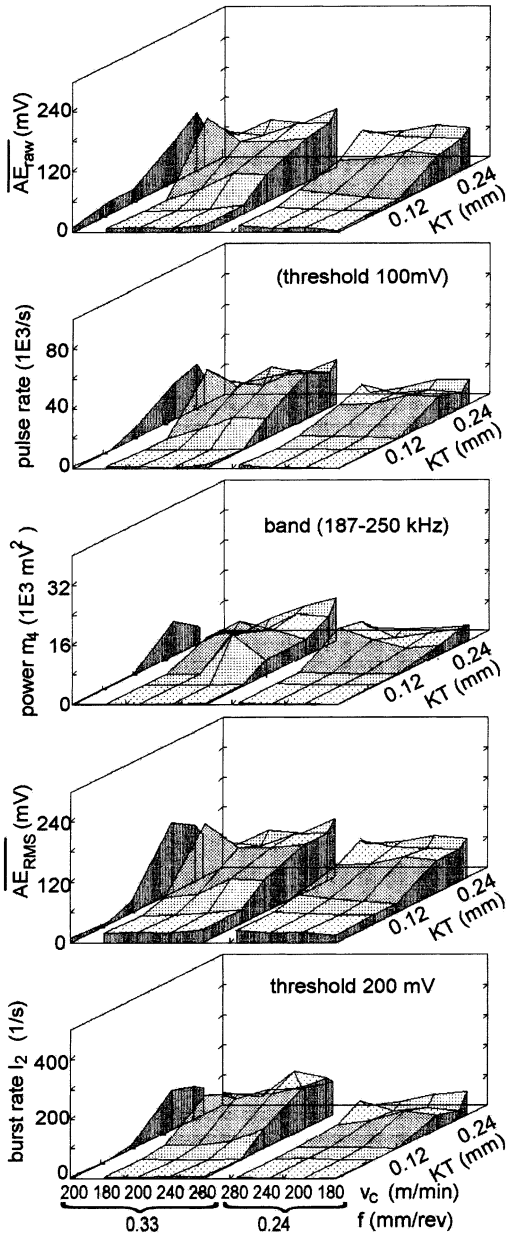

Fig. 7. AE measures dependence on tool wear (KT) for various cutting speeds (v_c) and feeds (f).

Table 1
Correlation coefficients between AE measures and crater depth (KT)

$\overline{AE}_{raw}$	s_{raw}	pr_1	pw_1	pr_2	pw_2	pr_3	pw_3
0.894	0.876	**0.669**	0.661	0.652	0.647	0.643	0.636
	m_2	m_3	m_4	m_5	m_6	m_0	
	0.790	0.764	0.813	**0.877**	0.751	0.833	
$\overline{AE}_{RMS}$	s_{RMS}	br_1	bw_1	br_2	bw_2	br_3	bw_3
0.904	0.903	**0.931**	0.922	0.928	0.930	0.928	0.923

Table 2
Correlation coefficients between AE measures

	br_1	$\overline{AE}_{RMS}$	m_5	pr_1	$\overline{AE}_{raw}$
$\overline{AE}_{raw}$	0.719	**0.991**	0.914	0.967	1
pr_1	0.583	**0.976**	0.846	1	
m_5	0.685	**0.898**	1		
$\overline{AE}_{RMS}$	**0.647**	**1**			
br_1	1				

denotes that either a measure is poorly correlated with the tool wear or there is a great influence of the cutting parameters on it. Reduction of this influence could increase the r value. However, indifference to the parameters is a positive feature. For AE_{raw} the best measures are $\overline{AE}_{raw}$, pr_1 or m_5. However, the best of all are demodulated AE measures: $\overline{AE}_{RMS}$ and br_1. Analysed AE measures are visibly (see Fig. 7) convergent regardless of different units and maximum values. The appropriate correlation coefficients between AE measures are given in Table 2. Assuming e.g. $\overline{AE}_{RMS}$ as a tool wear indicator excludes almost all other measures as highly correlated with $\overline{AE}_{RMS}$. Only burst rate for threshold 100 mV (br_1) is less correlated with $\overline{AE}_{RMS}$ and even better correlated with the crater depth. Since the AE_{RMS} is much easier to handle than AE_{raw}, these two ($\overline{AE}_{RMS}$ and br_1) can be recommended for tool condition monitoring. Usually the former is used, although the burst rate can be more advantageous as it is less disrupted by accidental amplifier overload and signal saturation.

4. Detection of catastrophic tool failure

Detection of catastrophic tool failure (chipping and breakage of the cutting tool) plays an important role in improving reliability and promoting automation of manufacturing processes. Many approaches have been proposed to accomplish this and some are successfully employed in industry. According to most of the research works, since a high amplitude peak (burst) of the AE signal is generated as a result of catastrophic tool failure, the magnitude of the AE_{RMS} signal has been considered as a useful mean of CTF detection [7]. Similar results were obtained from some of the experiments conducted in WUT. However, it has been found in some other

cases that the change in the AE_{RMS} value at the moment of tool failure is not significant, especially during interrupted cutting. The engagement of the cutting tool with the work material can generate AE signals of high amplitude, which can conceal useful signals normally generated by the tool breakage – see Fig. 8. Here a large burst of AE is generated at 15.51 s. i.e. 10 ms after the common burst generated by tool engagement. This can be attributed to a primary (initiative) tool failure. However, it is still not strong enough to be distinguished from other bursts. After about one revolution of the workpiece the failure is revealed, causing a characteristic [8] rise in the passive force F_p. However, there is no significant change in the AE_{RMS} signal value at this moment. Nevertheless a distinct change in the shape of AE_{RMS} signal after the CTF has occurred. It can be revealed by means of the central moments of the distribution function, the skew (the third central moment) and the kurtosis (the fourth central moment), assuming a β distribution of the AE_{RMS} signal [9]. Because high amplitude AE bursts often accompany the tool engagement, the number of data points per sample should contain data from at least one full revolution of the workpiece, see Fig. 9. Since the resulting measures from the distributions were obtained by the end of each individual sample, a delay of the CTF detection, usually close to the time span of one workpiece revolution, is inevitable. In the case presented in Fig. 9, a cutting edge chipping has occurred at about 13.7 s, causing a marked change of the cutting force signal. It can be noticed that not only was there no significant burst of AE at the instant of the CTF, but also the burst usually accompanying the tool entrance was even smaller. An abrupt change in kurtosis of β distribution (K_B) value has occurred at about 0.18 s after CTF caused a change of the feed force F_f. Moreover all the disturbances appeared in the AE_{RMS} course due to tool engagement with work material are undetectable in the K_B course.

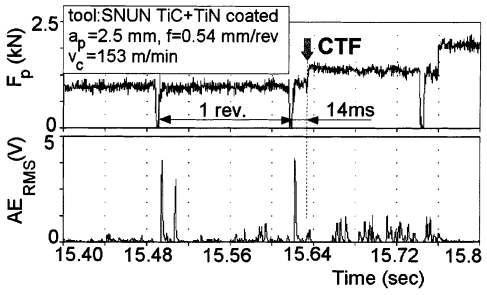

Fig. 8. AE_{RMS} signal course in the case of CTF during interrupted cutting.

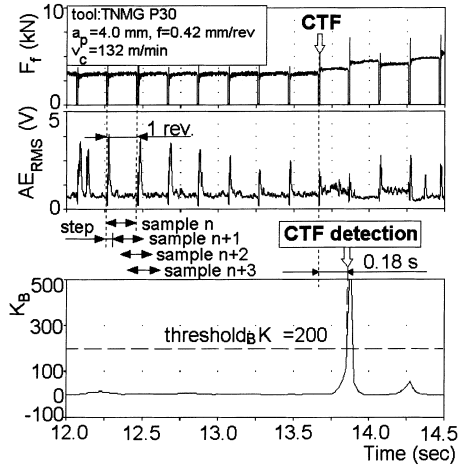

Fig. 9. Suitability of CTF detection by kurtosis of AE_{RMS} signal β distribution.

70 cutting tests were carried out, in which 51 cases of CTF have occurred. After analysis of all tests it appeared that, if $K_B = 200$ were used as a detection threshold, 45 instances of CTF would be detected.

5. Conclusions

1. The AE buffer amplifier gain should be as small as possible to avoid its overload and distortion of the signal. Any further necessary signal amplification should be carried out after high-pass filtering.
2. Average value of AE_{RMS} and burst rate are simple AE signal measures best suited for tool wear assessment in turning.
3. The kurtosis of β distribution of the AE_{RMS} signal were found to exhibit good sensitivity to the tool breakage and chipping which make them promising symptoms for the CTF monitoring.

References

[1] G. Byrne, D. Dornfeld, I. Inasaki, G. Ketteler, W. König, R. Teti, Ann. CIRP 44 (1995) 541.
[2] K. Jemielniak, J. Kosmol, in: Proceedings VI CIRP Workshop on Supervising and Diagnostics of Machining Systems, Karpacz, Poland (1995) 90.
[3] K. Jemielniak, in: AC'98, Proceedings V CIRP International Conference on Monitoring and Automatic Supervision in Manufacturing, Miedzeszyn, Poland (1998) 90.
[4] H.V. Ravindra, Y.G. Srinivasa, R. Krishnamurty, Wear 212 (1999) 78.
[5] K. Jemielniak, O. Belgassim, in: Proc. VII CIRP Workshop on Supervising and Diagnostics of Machining Systems, Karpacz, Poland (1996) 241.
[6] K. Jemielniak, L. Kwiatkowski, P. Wrzosek, J. Intell. Manuf. 9 (1998) 447.
[7] M. Lan, D. Dornfeld, Trans. ASME, J. Eng. Mater. Technol. 106 (1984) 111.
[8] K. Jemielniak, Ann. CIRP 41 (1992) 97.
[9] K. Jemielniak, O. Otman, Ann. CIRP 47 (1998) 31.